NASA TECHNICAL NOTE

NASA TN D-2797

NASA TN D-2797

PARAMETRIC INVESTIGATION OF LIQUID HYDROGEN TANK PRESSURIZATION DURING OUTFLOW

by David A. Mandell and William H. Roudebush

Lewis Research Center
Cleveland, Ohio

NATIONAL AERONAUTICS AND SPACE ADMINISTRATION • WASHINGTON, D. C. • APRIL 1965

NASA TN D-2797

PARAMETRIC INVESTIGATION OF LIQUID HYDROGEN TANK PRESSURIZATION DURING OUTFLOW

By David A. Mandell and William H. Roudebush

Lewis Research Center
Cleveland, Ohio

NATIONAL AERONAUTICS AND SPACE ADMINISTRATION

For sale by the Clearinghouse for Federal Scientific and Technical Information
Springfield, Virginia 22151 – Price $2.00

PARAMETRIC INVESTIGATION OF LIQUID HYDROGEN TANK PRESSURIZATION DURING OUTFLOW

by David A. Mandell and William H. Roudebush

Lewis Research Center

SUMMARY

The factors influencing the amount of gas required to pressurize a cylindrical tank of liquid hydrogen during outflow are investigated analytically based on a simplified model of the tank-flow and heat-transfer problem. The investigation begins with an established set of differential equations describing the problem. These equations and associated initial and boundary conditions are put in terms of dimensionless variables. The ratio of the mass of gas required for pressurization to a standard mass is shown to depend on only a few parameters. By computer solution of the equations over a wide range of values of the parameters it is found that only two are of principal importance. These two dimensionless parameters have the form of modified Stanton numbers, one associated with the gas and one with the tank wall. A figure is presented from which the pressurant mass ratio can be found for a wide range of values of the modified gas and wall Stanton numbers. A comparison with experimental results is made.

INTRODUCTION

Liquid hydrogen is now established as a rocket fuel. However, the design of new hydrogen rocket systems will require a better understanding of the thermal processes occurring inside the hydrogen tank. The particular problem treated here is the prediction of the amount of pressurizing gas that must be added to the tank to maintain a desired pressure during outflow of the fuel.

A one-dimensional analysis of the nonsteady heat-transfer and flow problem for a cylindrical tank during outflow was given in reference 1. A numerical method was presented there for calculating the temperature distribution in the tank, from which the amount of pressurizing gas that must be supplied during outflow can be obtained. Calculated results in reference 1 were compared with experimental data. The agreement

was sufficiently good to suggest the use of the method for an analytical investigation of the various parameters influencing the pressurant requirement.

Such an investigation is described in this report. It is shown that the important factors entering the pressurization problem can be combined into a small number of parameters. These parameters are then varied over a wide range and their effect on mass requirements is obtained.

The analytical results presented herein extend far beyond the range where the theory of reference 1 has been checked against experimental data. Furthermore, some complicating factors such as liquid sloshing and tank dome heating are ignored. Nevertheless, it is hoped that the results will give at least a reliable estimate of the effects of the most important pressurization parameters for cylindrical tanks and help in preliminary design.

ANALYSIS

Assumptions

The following parametric analysis of the pressurization problem is based on the equations of reference 1. In that reference a simple flow model was constructed based on the following assumptions:

(1) The ullage gas is nonviscous.

(2) The ullage gas velocity is everywhere parallel to the tank axis and does not vary radially or circumferentially.

(3) The tank pressure does not vary spatially.

(4) The ullage gas temperature does not vary radially or circumferentially.

(5) The tank wall temperature does not vary radially or circumferentially.

(6) No heat is transferred axially in either the gas or the wall.

(7) No condensation or evaporation occurs.

(8) No heat is transferred at the liquid interface or at the top of the tank.

With these assumptions the problem reduces to a one-dimensional nonsteady flow problem with heat addition. The governing fluid dynamic and heat-transfer equations are given in reference 1.

Some further assumptions are made in the present report. These added restrictions allow the differential equations and the initial and boundary conditions to be put into a simple form that clearly exhibits the significant dimensionless groups. Later in the report an examination is made of the effect of these assumptions:

(9) The ullage gas is a perfect gas with constant specific heat.

(10) The inlet gas temperature, the tank pressure, and the outflow rate are constant.

(11) The gas-to-wall heat-transfer coefficient is constant.

(12) The gas and wall temperatures at the start of outflow are equal and vary linearly in the direction of the tank axis from saturation temperature at the liquid interface to one-half the sum of the saturation temperature and the inlet gas temperature at the top of the tank.

(13) The gas and wall temperatures at the liquid interface are constant and equal throughout the outflow period.

Differential Equations and Initial and Boundary Conditions

A schematic drawing of a cylindrical tank is shown in figure 1. With the added assumptions (9) to (13) the equations of reference 1 for such a tank reduce to

$$\frac{DT}{Dt} = \frac{2hR}{rMPc_p}(T_w - T)T \tag{1}$$

$$\frac{\partial T_w}{\partial t} = \frac{h}{\ell_w \rho_w c_w}(T - T_w) \tag{2}$$

$$\frac{\partial u}{\partial x} = \frac{2hR}{rMPc_p}(T_w - T) = \frac{1}{T}\frac{DT}{Dt} \tag{3}$$

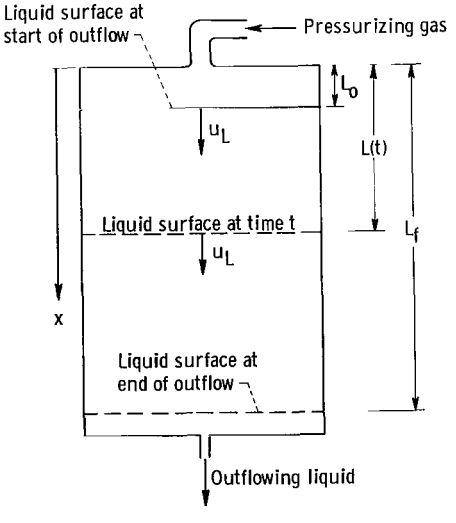

Figure 1. - Schematic of cylindrical liquid-propellant tank during outflow.

All symbols are defined in the appendix. The detailed development of these equations and a discussion of the underlying assumptions (1) to (8) are given in reference 1, along with a comparison of calculated and experimental results.

Let L(t) denote the x-location of the liquid surface at time t (see fig. 1). The velocity u_L of the surface is constant since the outflow rate has been assumed constant. Therefore,

$$L(t) = L_o + u_L t \tag{4}$$

where $L_o \equiv L(0)$ is the axial length of the ullage at the start of outflow.

From assumption (12) the initial conditions can be written as

$$T = T_w = \frac{T_L + T_g}{2} + \frac{x}{L_o}\left(\frac{T_L - T_g}{2}\right) \qquad t = 0 \qquad 0 \leqq x \leqq L_o \tag{5}$$

This choice of initial temperatures is arbitrary. In an actual example the initial gas and wall temperatures need not be equal and need not relate in any way to T_g. The effect of the choice will be examined later in the report.

The gas temperature at the top of the tank during outflow is

$$T = T_g = \text{constant} \qquad x = 0 \qquad 0 < t \leqq t_f \tag{6}$$

The gas and wall temperatures at the liquid surface are

$$T = T_w = T_L = \text{constant} \qquad x = L_o + u_L t \qquad 0 < t \leqq t_f \tag{7}$$

and the velocity of the gas is

$$u = u_L = \text{constant} \qquad x = L_o + u_L t \qquad 0 < t \leqq t_f \tag{8}$$

Equations (1) to (8) completely determine the problem.

Dimensionless Equations

The preceding equations will now be made dimensionless by introducing the following dimensionless variables:

$$\left.\begin{aligned} \hat{t} &= \frac{t}{t_f} \\ \hat{x} &= \frac{x}{L_f - L_o} \\ \hat{u} &= \frac{u}{u_L} \\ \hat{T} &= \frac{T}{T_g} \\ \hat{T}_w &= \frac{T_w}{T_g} \end{aligned}\right\} \tag{9}$$

Since the velocity of the liquid surface is constant,

$$L_f - L_o = u_L t_f \tag{10}$$

Using equations (9) and (10) in equations (1) to (8) yields the following equations:

$$\frac{D\hat{T}}{D\hat{t}} = \frac{2hRt_f T_g}{rMPc_p}(\hat{T}_w - \hat{T})\hat{T} \tag{11}$$

$$\frac{\partial \hat{T}_w}{\partial \hat{t}} = \frac{ht_f}{\ell_w \rho_w c_w}(\hat{T} - \hat{T}_w) \tag{12}$$

$$\frac{\partial \hat{u}}{\partial \hat{x}} = \frac{1}{\hat{T}} \frac{D\hat{T}}{D\hat{t}} \tag{13}$$

$$\hat{L}(\hat{t}) = \hat{L}_o + \hat{t} \tag{14}$$

$$\hat{T} = \hat{T}_w = \frac{\hat{T}_L + 1}{2} + \frac{\hat{x}}{\hat{L}_o} \frac{\hat{T}_L - 1}{2} \qquad \text{for } \hat{t} = 0,\ 0 \leqq \hat{x} \leqq \hat{L}_o \tag{15}$$

$$\hat{T} = 1 \qquad \text{for } \hat{x} = 0,\ 0 < \hat{t} \leqq 1 \tag{16}$$

$$\hat{T} = \hat{T}_w = \hat{T}_L \qquad \text{for } \hat{x} = \hat{L}_o + \hat{t},\ 0 < \hat{t} \leqq 1 \tag{17}$$

$$\hat{u} = 1 \qquad \text{for } \hat{x} = \hat{L}_o + \hat{t},\ 0 < \hat{t} \leqq 1 \tag{18}$$

When the perfect gas equation of state and equation (10) are used, the group of quantities appearing in equation (11) can be written as a modified Stanton number:

$$\frac{hRt_f T_g}{rMPc_p} = \frac{ht_f}{r\rho_g c_p} = \frac{h}{\hat{r}\rho_g c_p u_L} = St_g \tag{19}$$

The modified gas Stanton number St_g is a true Stanton number modified by division by the dimensionless radius $\hat{r}$.

In connection with equation (12) a second modified Stanton number related to the wall

and called the modified wall Stanton number is defined as

$$St_w = \frac{ht_f}{\ell_w \rho_w c_w} = \frac{h}{\hat{\ell}_w \rho_w c_w u_L} \tag{20}$$

Although St_w has the form of a Stanton number, properties of both wall and fluid are involved. The use of such a dimensionless group is unusual. An alternative is to replace St_w by the parameter

$$\frac{St_g}{St_w} = \frac{\ell_w \rho_w c_w}{r \rho_g c_p}$$

which is one-half the ratio of the heat capacity of the wall to the heat capacity of the gas. However, St_w has been retained in this analysis since it appeared naturally in the differential equation.

An examination of equations (11) to (20) reveals that the set of dimensionless differential equations and the initial and boundary conditions depend only on the four dimensionless quantities St_g, St_w, $\hat{L}_o$, and $\hat{T}_L$. With the assumptions previously made for this analysis, St_g, $\hat{L}_o$, and $\hat{T}_L$ are constant for a particular problem. If, furthermore, c_w can be considered constant, the following result is obtained: Every solution of the pressurization problem in terms of the dimensionless variables (eq. (9)) is completely determined by the specification of the four dimensionless constants St_g, St_w, $\hat{L}_o$, and $\hat{T}_L$.

In dealing with liquid hydrogen problems the wall specific heat variation may be significant. In that case the parameter St_w will vary, also. In order to maintain St_w as a characteristic constant of the problem, it is convenient to introduce some reference value of specific heat $\bar{c}_w$ constant for a given problem. To do this equation (20) is modified in the following way:

$$\frac{h}{\hat{\ell}_w \rho_w c_w u_L} = \frac{h}{\hat{\ell}_w \rho_w \bar{c}_w u_L} \frac{\bar{c}_w}{c_w} = St_w \hat{c}_w \tag{21}$$

where

$$\hat{c}_w \equiv \frac{\bar{c}_w}{c_w} \tag{22}$$

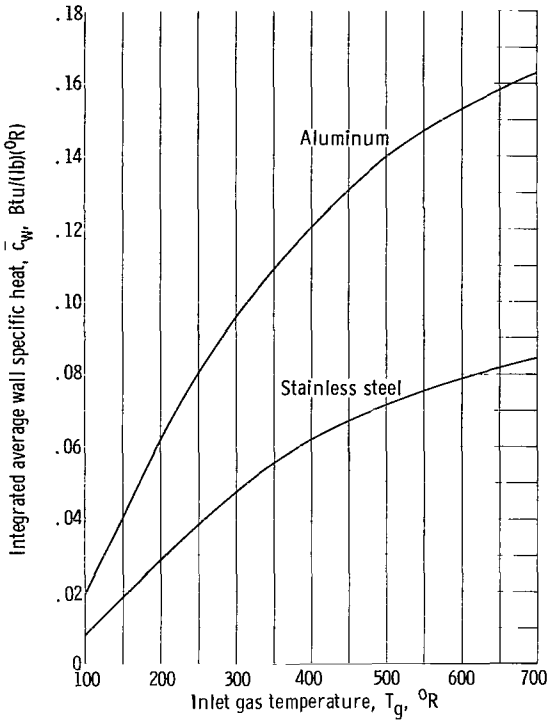

Figure 2. - Integrated average wall specific heats used to calculate wall Stanton numbers for stainless-steel and aluminum tanks.

In equation (21) the parameter St_w is constant for a given problem, and the variation of wall specific heat is accounted for in the new dimensionless variable $\hat{c}_w$. The reference specific heat $\bar{c}_w$ can be chosen arbitrarily; for example, a value at room temperature could be used. However, the use of an appropriate average value would be expected to reduce the effect of the variable $\hat{c}_w$. In this report the following value is used:

$$\bar{c}_w \equiv \frac{1}{T_g - 37} \int_{37}^{T_g} c_w(T)dT$$

A plot of $\bar{c}_w$ against T_g is given in figure 2 for stainless steel and aluminum.

When equation (21) is used, the problem is seen to depend on the four dimensionless constants St_g, St_w, $\hat{L}_o$, and $\hat{T}_L$ and the dimensionless specific heat variation $\hat{c}_w$.

The specific heat variation $\hat{c}_w$ can be expected to vary differently with different tank wall materials and thereby produce different results. Therefore, attention will be confined largely to a single tank wall material, stainless steel. Even when this is done, however, a difficulty remains. The variation $\hat{c}_w$ is a function of the dimensional variable T_g as well as the dimensionless variable $\hat{T}$. Thus, the following result can be formulated: For a given wall material every solution of the pressurization problem in terms of the dimensionless variables of equation (9) is completely determined by the specification of four dimensionless constants St_g, St_w, $\hat{L}_o$, and $\hat{T}_L$ and the one-dimensional constant T_g.

Mass Ratio

A solution of the dimensionless pressurization equations gives $\hat{T}$, $\hat{T}_w$, and $\hat{u}$ as functions of $\hat{x}$ and $\hat{t}$. When the assumption of a perfect gas is used, the total mass of pressurizing gas added during outflow is given by

$$m = \int_0^{L_f} \pi r^2 \rho(x, t_f)dx - \int_0^{L_o} \pi r^2 \rho(x, 0)dx$$

$$= \frac{\pi r^2 MP}{R}\left[\int_0^{L_f} \frac{dx}{T(x, t_f)} - \int_0^{L_o} \frac{dx}{T(x, 0)}\right]$$

$$= \frac{\pi r^2 MP(L_f - L_o)}{RT_g}\left[\int_0^{\hat{L}_f} \frac{d\hat{x}}{\hat{T}(\hat{x}, 1)} - \int_0^{\hat{L}_o} \frac{d\hat{x}}{\hat{T}(\hat{x}, 0)}\right] \tag{23}$$

If the ideal pressurant mass m_i is defined to be the mass required to pressurize the tank if no heat transfer occurs, then

$$m_i = \pi r^2(L_f - L_o)\rho_g = \frac{\pi r^2 MP(L_f - L_o)}{RT_g} \tag{24}$$

Combining equations (23) and (24) gives

$$\frac{m}{m_i} = \int_0^{\hat{L}_f} \frac{d\hat{x}}{\hat{T}(\hat{x}, 1)} - \int_0^{\hat{L}_o} \frac{d\hat{x}}{\hat{T}(\hat{x}, 0)} \tag{25}$$

The dimensionless temperature variation $\hat{T}(\hat{x}, \hat{t})$ appearing in equation (25), and thereby the mass ratio m/m_i, is determined by the solution of the dimensionless equations. This mass ratio is sometimes referred to as a collapse factor in pressurization literature. As just shown it arises naturally from the choice of dimensionless variables in equation (9).

The mass ratio but not the mass itself is determined by the solution of the dimensionless equations. Determining the mass from the mass ratio requires also the displaced liquid volume $\pi r^2(L_f - L_o)$, the tank pressure, and the inlet gas temperature (see eq. (24)).

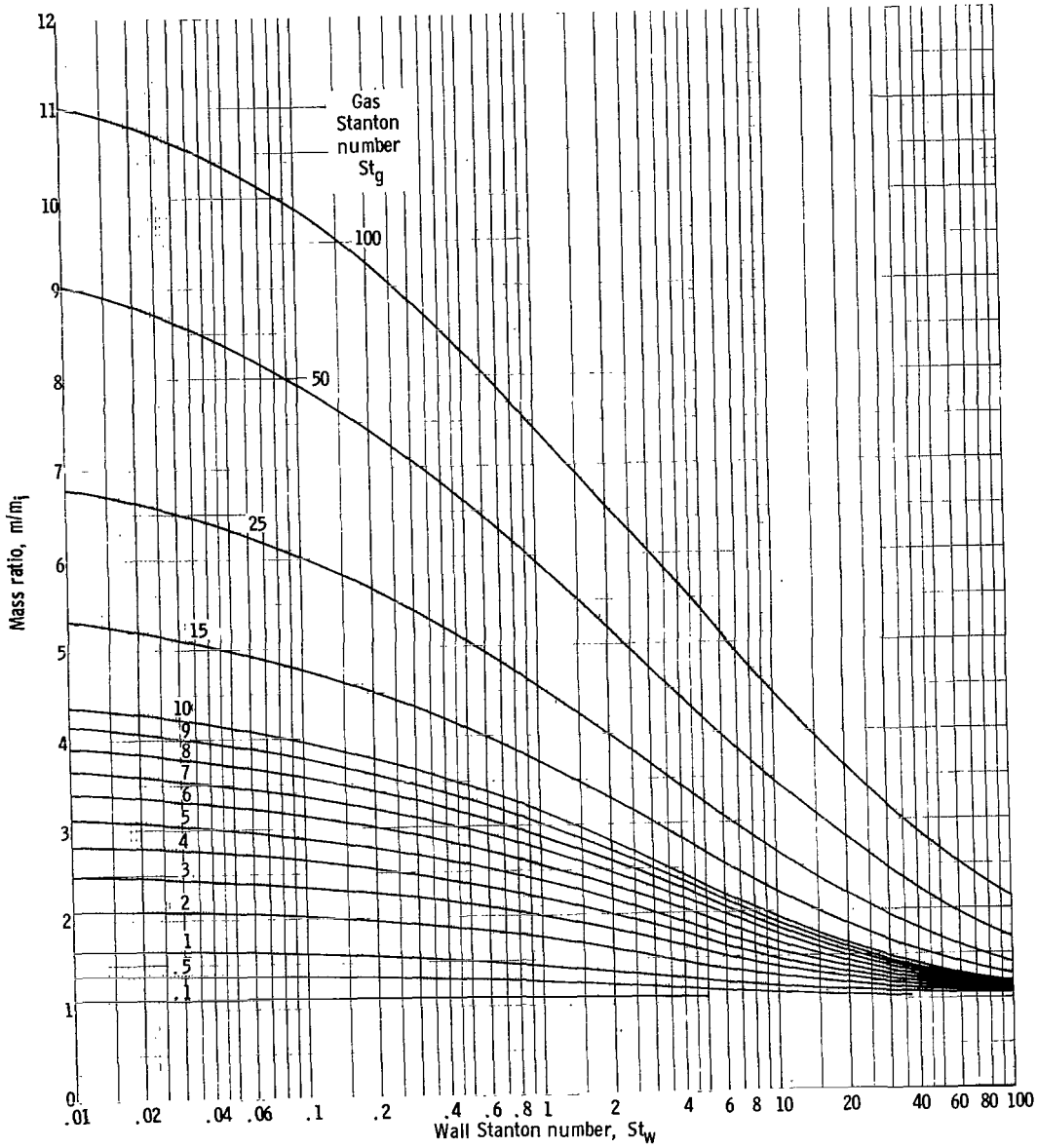

Figure 3. - Reference Stanton number map showing values of pressurant mass ratio for range of gas and wall modified Stanton numbers for cylindrical stainless-steel tanks. Inlet gas temperature, 500^0 R; liquid surface temperature, 37^0 R; dimensionless initial ullage height, 0.0526.

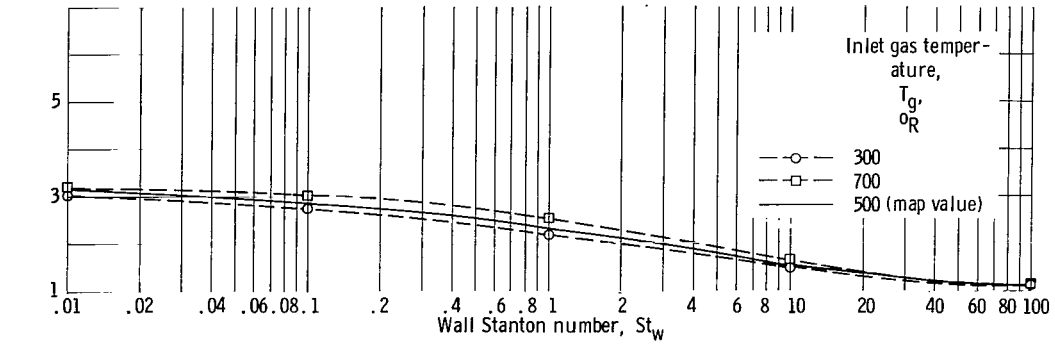

(a) Gas Stanton number, 5.

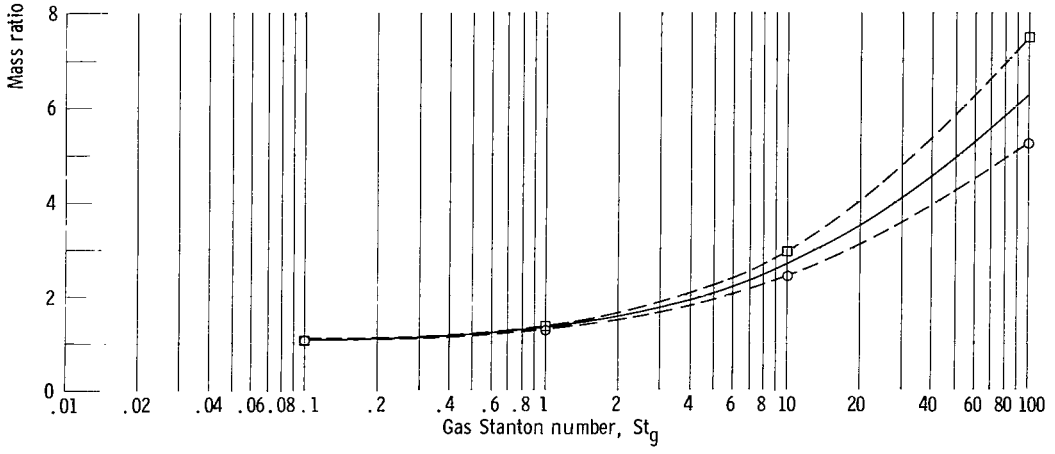

(b) Wall Stanton number, 2.5.

Figure 4. - Effect on mass ratio of changing the inlet gas temperature. Dimensionless interface temperature, 0.074; dimensionless initial ullage height, 0.0526.

RESULTS

As indicated in the previous section, the mass ratio m/m_i is completely determined by choosing a tank wall material and fixing values of the five constants St_g, St_w, $\hat{L}_o$, $\hat{T}_L$, and T_g. In the present section some quantitative results are presented for stainless-steel tanks.

First, with the computer solution described in reference 1, values of gas temperature distribution and thereby values of m/m_i are computed for a wide range of values of St_g and St_w by using fixed values of $\hat{L}_o$, $\hat{T}_L$, and T_g. Then with these results as a standard for comparison, additional calculations are made to examine the effect of $\hat{T}_g$, $\hat{T}_L$, and $\hat{L}_o$. Finally, some of the assumptions made to obtain the simple dimensionless equations are relaxed, and calculations are made to examine their effect.

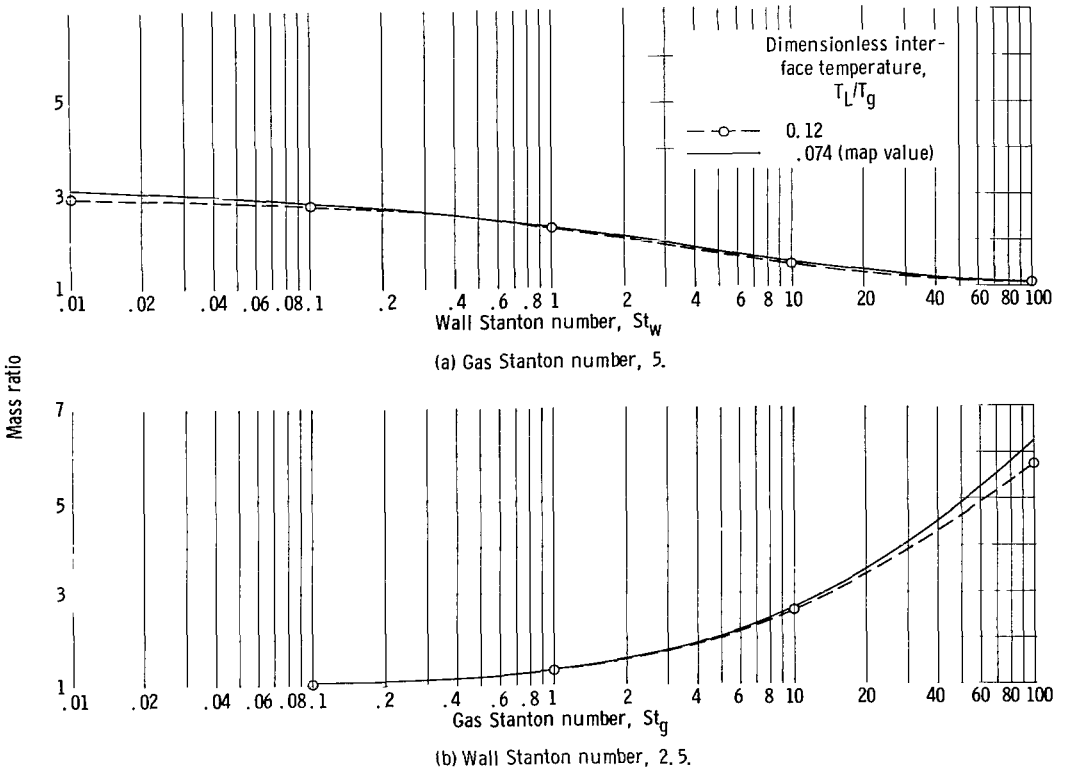

Figure 5. - Effect on mass ratio of changing the dimensionless interface temperature. Inlet gas temperature, 500° R; dimensionless initial ullage height, 0.0526.

Reference Stanton Number Map

The inlet gas temperature T_g is taken to be 500° R. The temperature $\hat{T}_L$ is chosen to be 0.074, corresponding to a liquid surface temperature of 37° R. Selection of a 5-percent initial ullage volume gives a value of $\hat{L}_o = 0.0526$. The effect of this choice of values for T_g, $\hat{T}_L$, and $\hat{L}_o$ will be examined later. With these values fixed, the mass ratio becomes a function only of the modified Stanton numbers. For each pair of values of St_g and St_w a computer solution can be carried out to obtain m/m_i.

The computed mass ratios for a wide range of Stanton numbers are shown in figure 3. This figure will be referred to as the reference Stanton number map. The map is intended to encompass existing experimental tanks and flight tanks that now exist or are likely to be developed. In the next section it is shown that the effects of T_g, $\hat{T}_L$, and $\hat{L}_o$ are relatively small so that figure 3 provides a rapid estimate of mass ratio for a wide variety of cylindrical tanks.

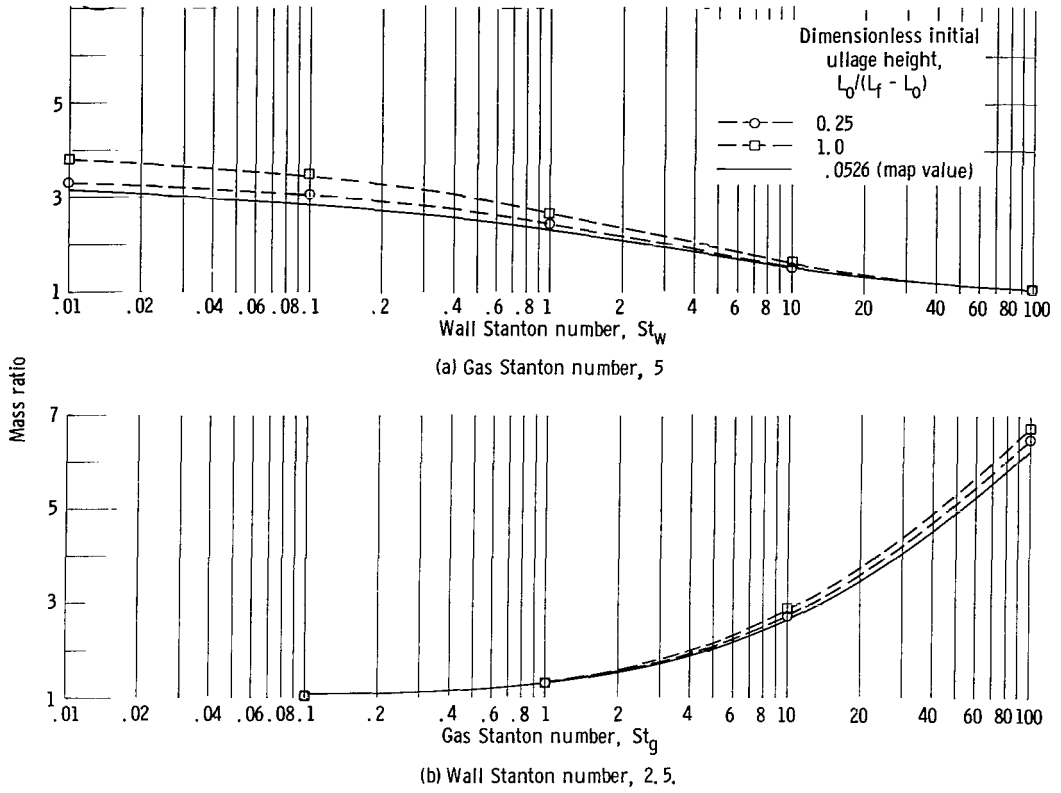

Figure 6. - Effect on mass ratio of changing the dimensionless initial ullage height. Inlet gas temperature, 500° R; dimensionless interface temperature, 0.074.

Effect of Parameters T_g, $\hat{T}_L$, and $\hat{L}_o$

When $\hat{L}_o$ and $\hat{T}_L$ are held fixed, the mass ratio depends only on T_g for fixed values of the gas and wall Stanton numbers. As previously explained, this dependence on T_g enters through the dependence of the wall specific heat ratio $\hat{c}_w$ on T_g. It might be expected therefore that the dependence is small. An indication of the effect of changing T_g from the value of 500° R used in the reference Stanton number map to 300° and 700° R is given in figure 4. At a value of $St_g = 5$ the maximum deviation from the reference map values of mass ratio is 7.1 percent. At higher values of St_g the deviation increases as shown.

The effect of changing $\hat{T}_L$ while holding $\hat{L}_o$ and T_g fixed at reference map values is shown in figure 5. To change $\hat{T}_L$ the liquid surface temperature T_L is changed from 37° to 60° R. The effect appears to be negligible except at large values of St_g.

A similar result is true for $\hat{L}_o$. Keeping $\hat{T}_L$ and T_g fixed at reference map values and changing $\hat{L}_o$ gives the result shown in figure 6. The difference in mass

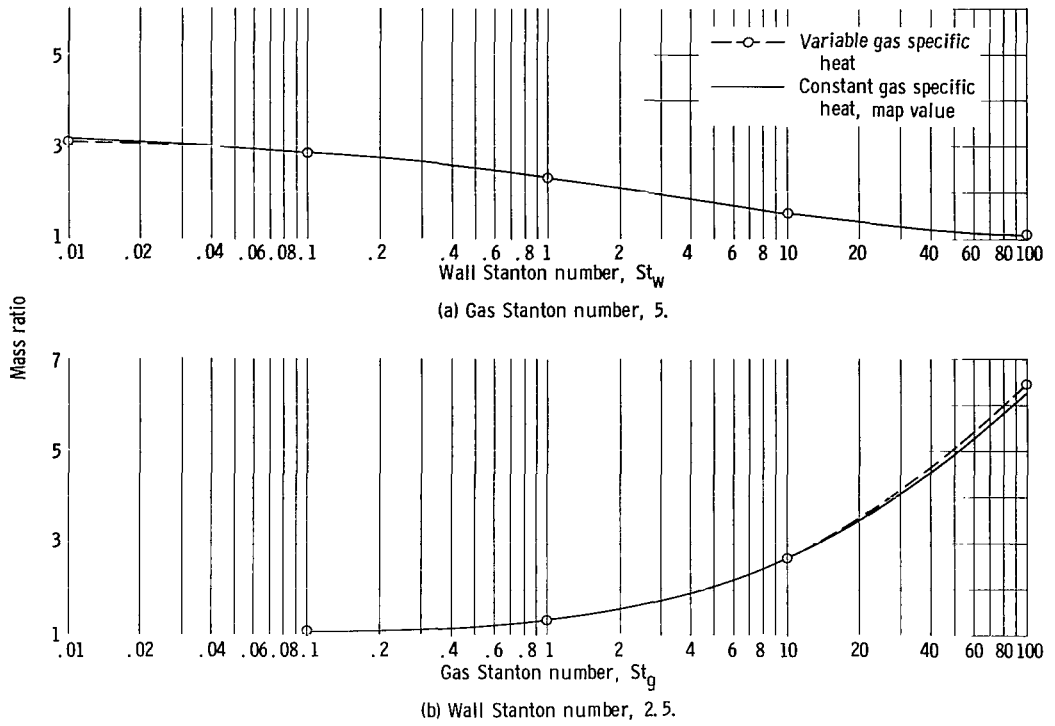

Figure 7. - Effect on mass ratio of allowing gas specific heat to vary with temperature. Inlet gas temperature, 500^0 R; dimensionless interface temperature, 0.074; dimensionless initial ullage height, 0.0526.

ratio brought about by changing the initial ullage volume from 5 to 20 percent is less than 7 percent over the range of Stanton numbers shown in the figure. When the initial ullage volume is increased to 50 percent, the maximum difference in mass ratio increases to about 14 percent.

These calculated results indicate that St_g and St_w are the primary factors affecting the mass ratio, at least for moderately small values of initial ullage.

Effect of Certain Assumptions

The effect of assuming gas specific heat to be constant was tested by computing mass ratios with a variable specific heat. In order to make a comparison with the values obtained for constant specific heat, it is necessary to assign a value of St_g to the cases where specific heat is allowed to vary. This is done by computing a mean $\bar{c}_p$ defined by

$$\bar{c}_p = \frac{1}{T_g - 37} \int_{37}^{T_g} c_p(T)dT$$

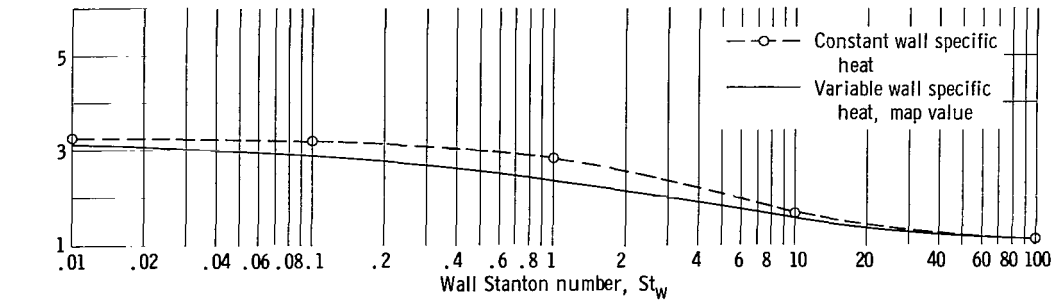

(a) Gas Stanton number, 5.

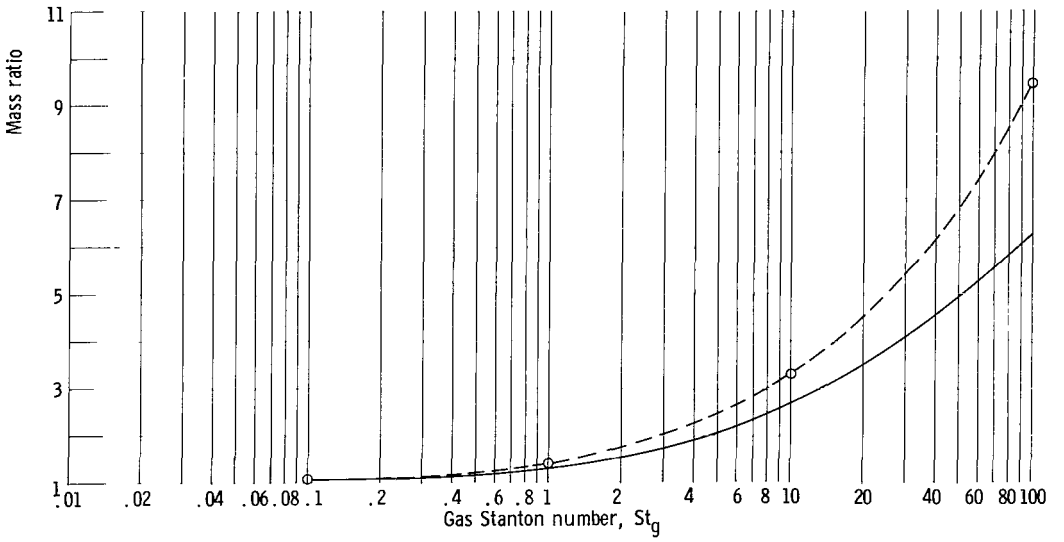

(b) Wall Stanton number, 2.5.

Figure 8. - Effect on mass ratio of holding wall specific heat constant. Inlet gas temperature, 500^0 R; dimensionless interface temperature, 0.074; dimensionless initial ullage height, 0.0526.

and by using it to determine St_g for each case. With this done the constant and varying specific heat cases can be compared at equal Stanton numbers. The results, shown in figure 7, indicate a negligible difference in mass ratios.

A variable wall specific heat was used to obtain the reference map (fig. 3). Figure 8 shows the effect of using instead a constant value of specific heat taken to be the integrated average value of figure 2. At $St_g = 5$ a maximum difference in mass ratio of 18.5 percent occurs at $St_w = 1$. Even larger differences occur at larger values of St_g. It was because of these large differences that the wall specific heat was allowed to vary for the reference map.

It is interesting, however, that changing the wall material from stainless steel to aluminum does not affect the mass ratio, as shown in figure 9. The reason for this is found in the near similarity of the variations $\hat{c}_w$ with $\hat{T}_w$ for the two metals (fig. 10).

Another assumption needed for the simplification of the dimensionless problem was that the wall and gas temperatures are equal and vary linearly with distance at the start

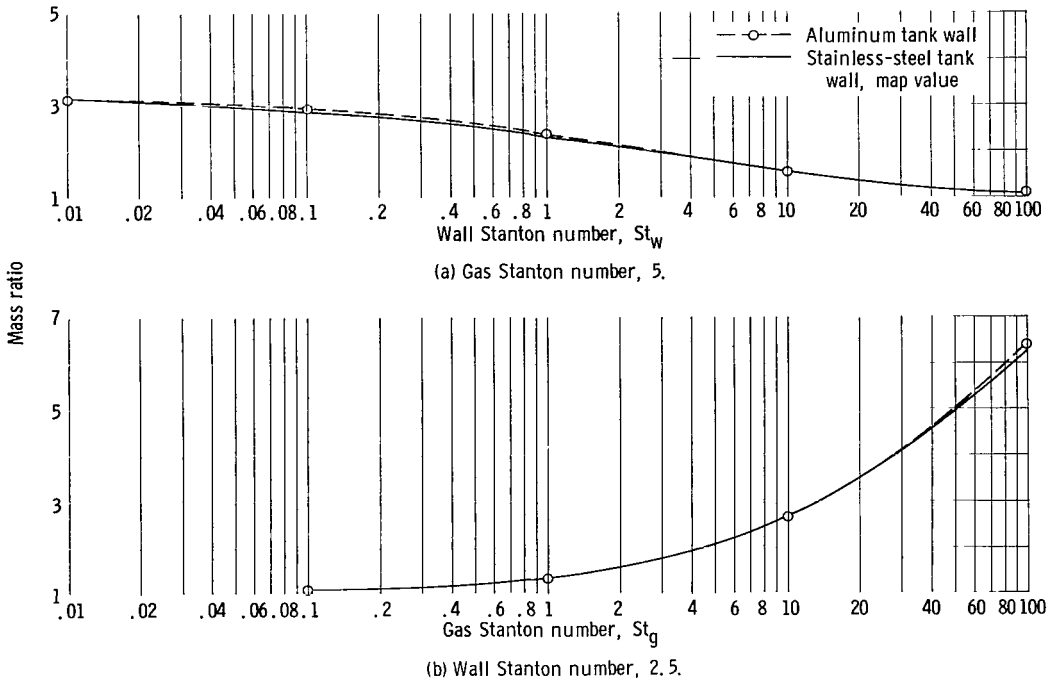

(a) Gas Stanton number, 5.

(b) Wall Stanton number, 2.5.

Figure 9. - Effect on mass ratio of changing tank wall material from stainless steel to aluminum. Dimensionless interface temperature, 0.074; dimensionless initial ullage height, 0.0526.

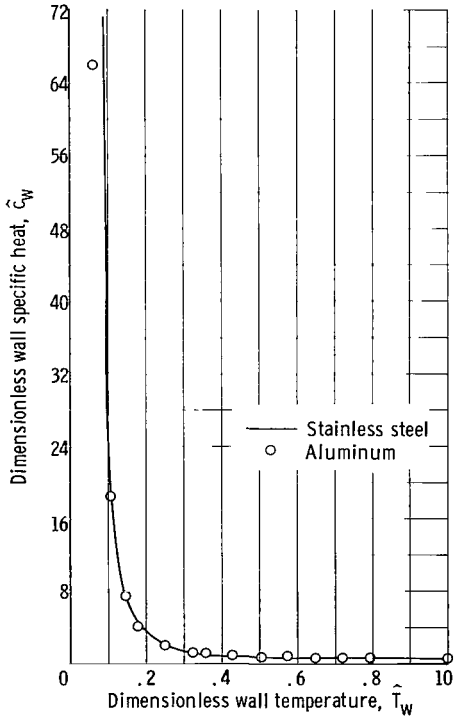

Figure 10. - Dimensionless wall specific heat as function of dimensionless wall temperature for stainless steel and aluminum. Inlet gas temperature, 500° R.

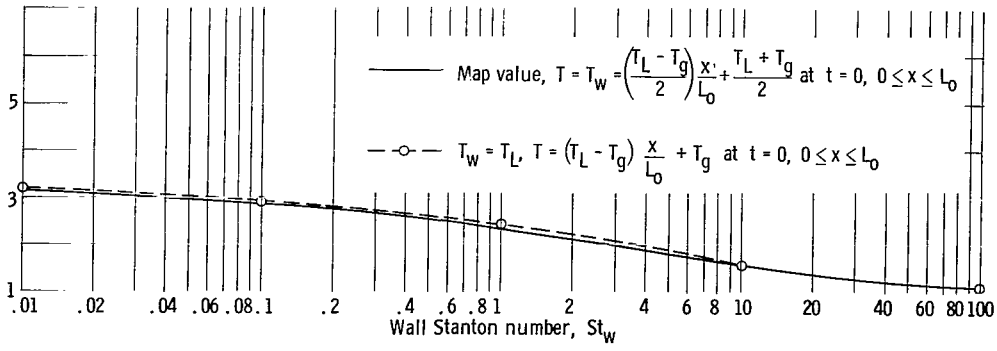

(a-1) Gas Stanton number, 5.

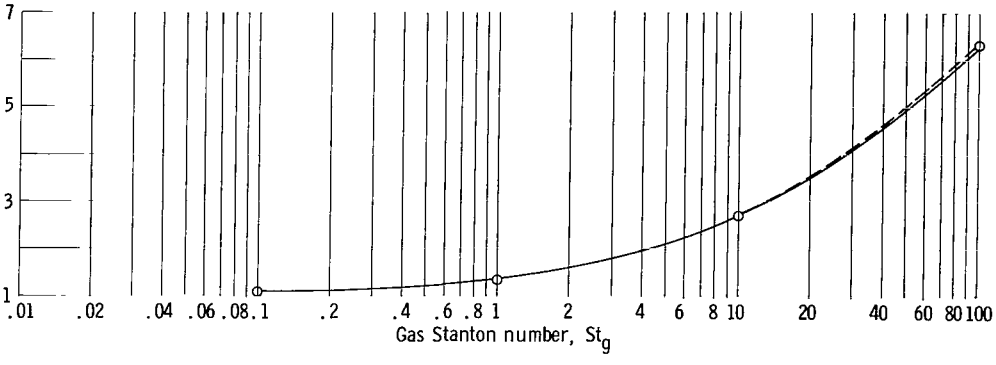

(a-2) Wall Stanton number, 2.5.

(a) Dimensionless initial ullage height, 0.0526.

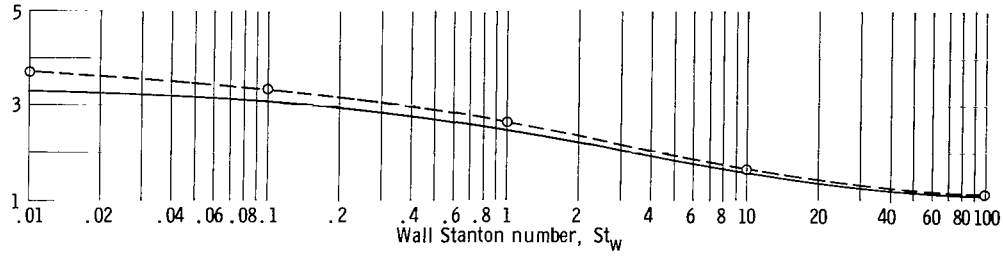

(b-1) Gas Stanton number, 5.

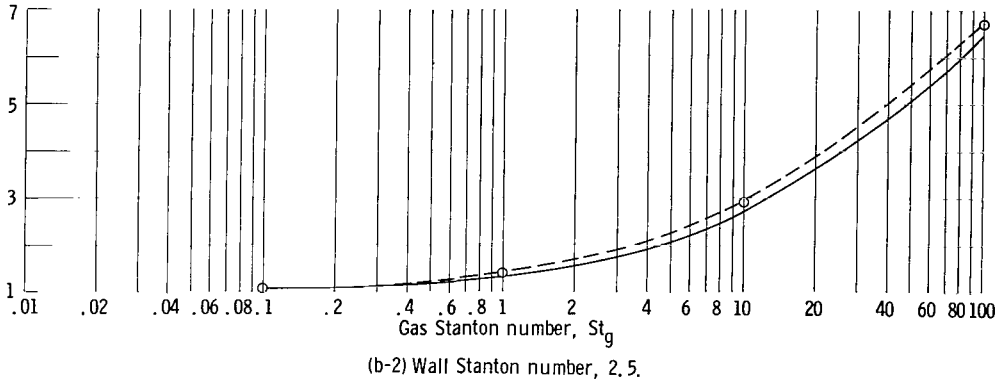

(b-2) Wall Stanton number, 2.5.

(b) Dimensionless initial ullage height, 0.25.

Mass ratio

Figure 11. - Effect on mass ratio of changing the assumed initial wall and gas temperatures. Dimensionless interface temperature, 0.074.

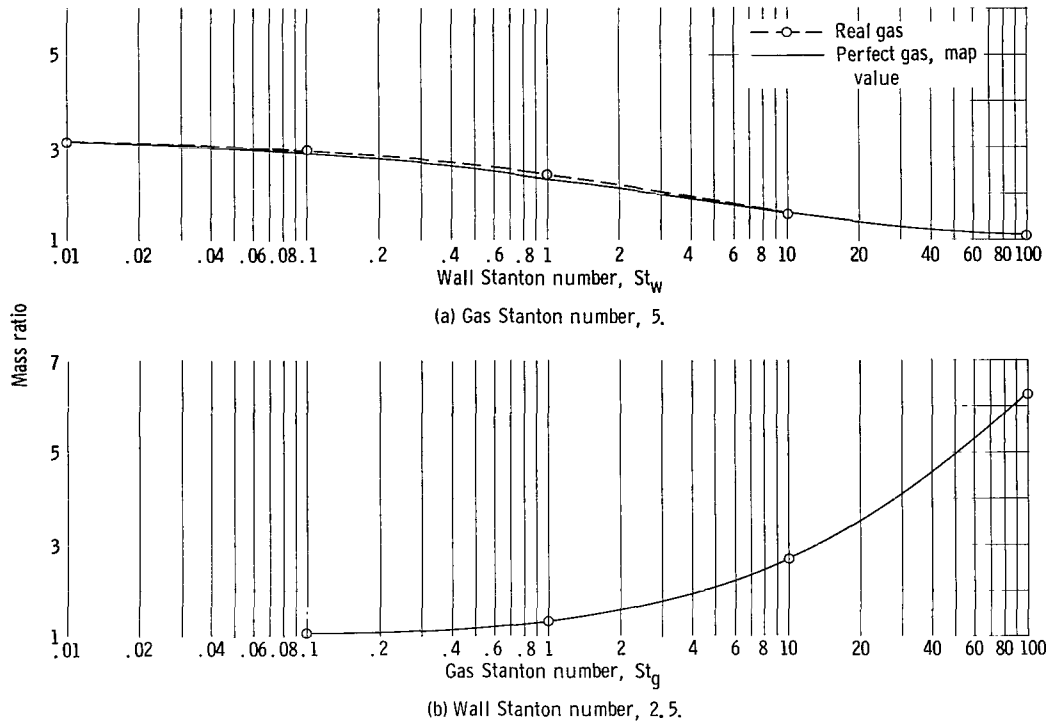

Figure 12. - Effect on mass ratio of considering a real gas. Inlet gas temperature, 500° R; dimensionless interface temperature, 0.074; dimensionless initial ullage height, 0.0526.

of outflow. In particular, they were assumed to vary from T_L at the liquid surface to $(T_L + T_g)/2$ at the top of the tank. Since the initial temperatures may not be easily computable in a particular case, this assumption assumes considerable importance.

To determine how critical the initial temperature distribution is, the following change in initial values was made. The initial wall temperature was taken to be 37° R at all points, and the gas temperature was varied linearly from 37° R at the liquid surface to 500° R at the top of the tank. The effect that this severe change in initial conditions had on the mass ratio is shown in figure 11. For initial ullage volumes of 5 percent (corresponding to values of $L_o/(L_f - L_o) = 0.0526$) the deviation from reference map values of mass ratio is negligible. At initial ullages of 20 percent the deviation is more significant, increasing to about 12 percent at $St_g = 5$ and $St_w = 0.1$.

The effect of assuming a perfect gas was also tested by using a real gas compressibility factor $Z(T, P)$ for hydrogen. The details of the equations needed in this case are given in reference 1. The results shown in figure 12 indicate that the difference in mass ratio brought about by using a real gas in the calculations is negligible.

It is difficult to evaluate the validity of the assumption of constant heat-transfer coefficient since the correct variation is not known for comparison. Reference 1 shows, however, that good agreement (within about 5 percent on the average) with experimental mass ratios can be obtained by using a constant value of h in the calculations. The

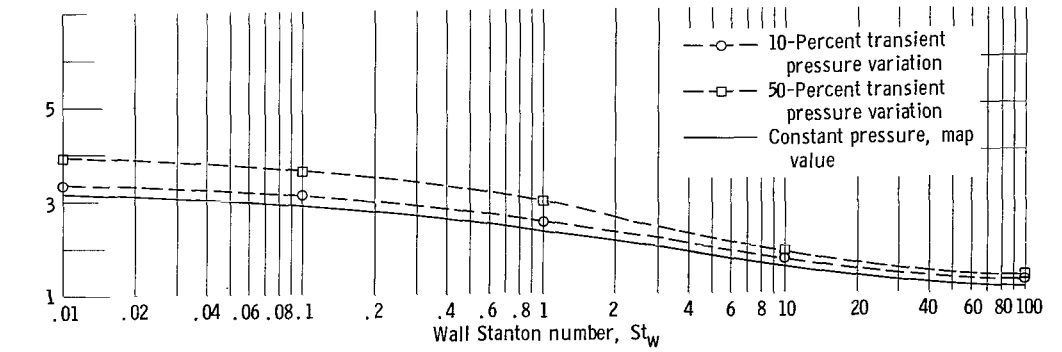

(a) Gas Stanton number, 5.

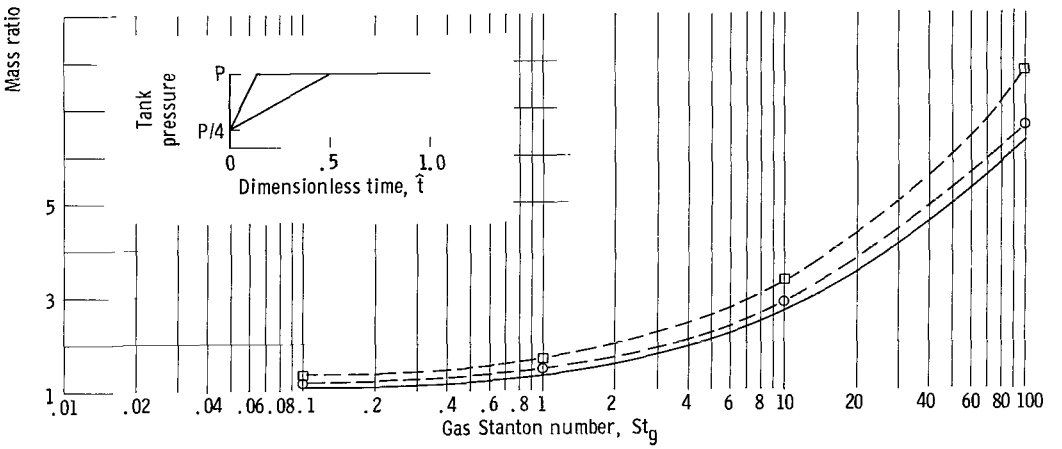

(b) Wall Stanton number, 2.5.

Figure 13. - Effect on mass ratio of transient tank pressure variations. Inlet gas temperature 500° R; dimensionless interface temperature, 0.074; dimensionless initial ullage height, 0.0526.

constant value used in each case in reference 1 was an average of experimentally measured local values of h.

The assumption of constant values of tank pressure, inlet gas temperature, and outflow rate will be violated to some extent in all real situations. In many cases, however, the deviation from constant values of these quantities will occur primarily during a starting transient. Figures 13, 14, and 15 show the effect on mass ratios of starting transients in tank pressure, inlet gas temperature, and outflow rate, respectively. Transients of 10 and 50 percent of total outflow time were considered. The magnitude of the transients are shown in each case in the respective figure.

The pressure transient has the most pronounced effect. The deviation, for all values of St_g and St_w, is about 25 percent for the 50-percent transient pressure variation and about 10 percent for the 10-percent transient.

For the 50-percent transient gas temperature variation, the deviation from the map value is approximately 14 percent at $St_g = 5$ and $St_w = 0.01$. This deviation decreases to 0 percent at $St_g = 5$ and $St_w = 100$. For $St_w = 2.5$, the deviation is approximately 14 percent at $St_g = 100$ and decreases to 1 percent at $St_g = 1$. The deviation is less

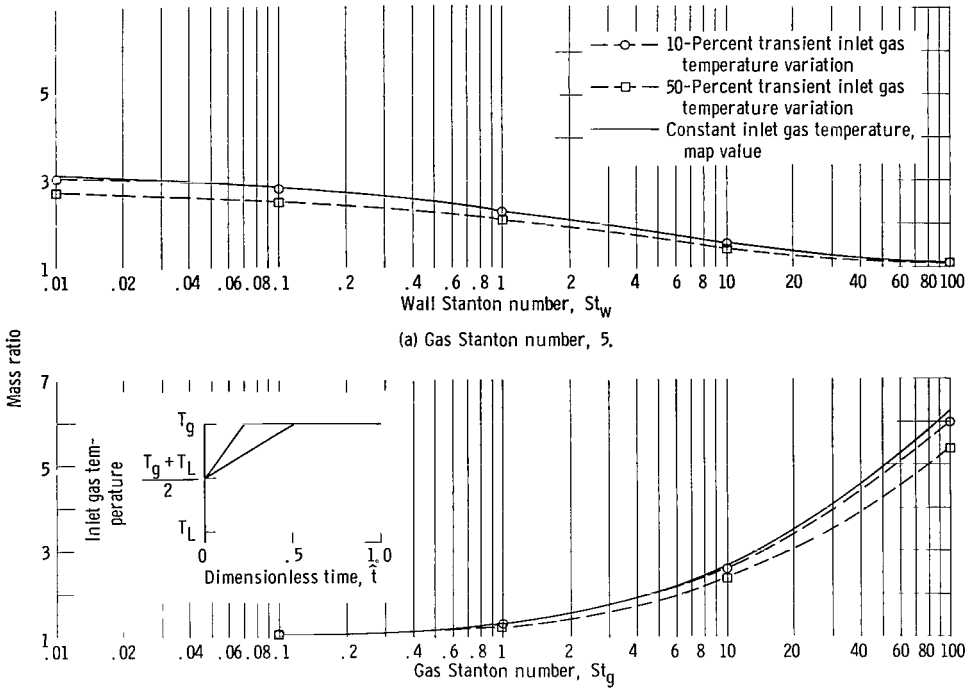

Figure 14. - Effect of transient inlet gas temperature variations. Inlet gas temperature, 500° R; dimensionless interface temperature, 0.074; dimensionless initial ullage height, 0.0526.

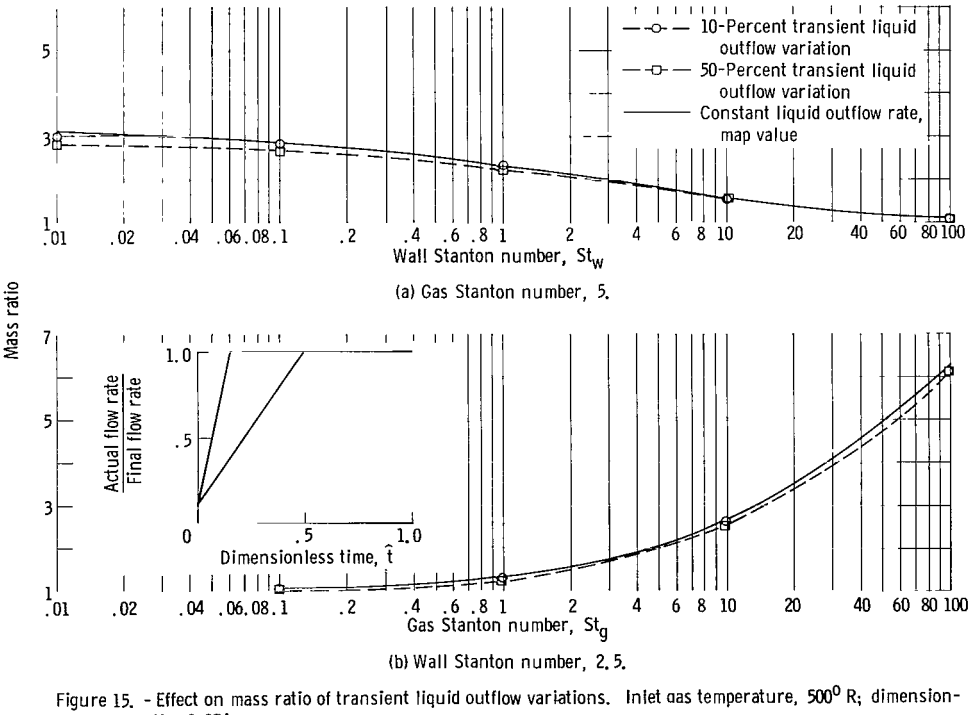

Figure 15. - Effect on mass ratio of transient liquid outflow variations. Inlet gas temperature, 500° R; dimensionless gas ratio, 0.074.

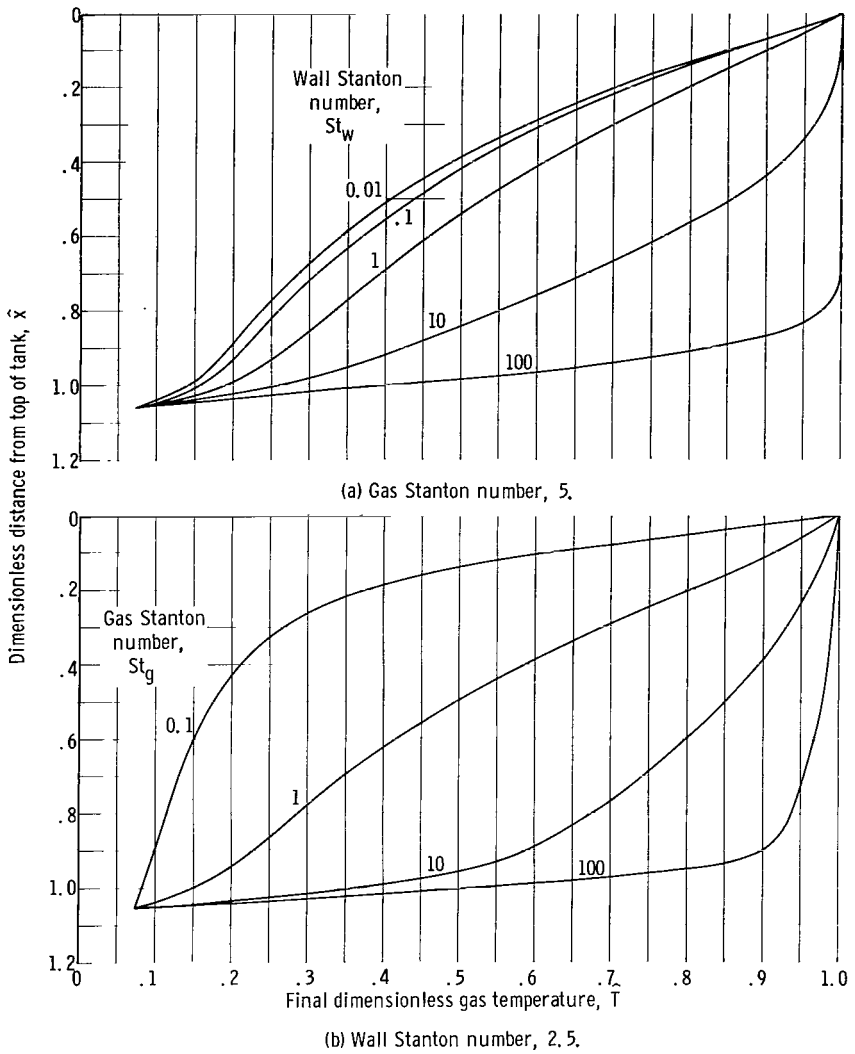

Figure 16. - Final dimensionless gas temperature variation at end of outflow. Dimensionless initial ullage height, 0.0526; dimensionless interface temperature, 0.074; dimensionless time from start of outflow, 1.

than 4 percent for the 10-percent transient.

The 50-percent transient liquid outflow variation deviates from the map a maximum of 8 percent. The 10-percent transient deviates about 2 percent.

Dimensionless Temperature Distributions

In addition to the propellant mass ratios, the dimensionless temperatures $\hat{T}_g$ and $\hat{T}_w$ are given as functions of $\hat{x}$ and $\hat{t}$ in the computer solutions. Figures 16 and 17 show the variety of shapes that can occur in the final gas and wall temperature profiles, respectively, obtained at various points of the Stanton number map. The assumption

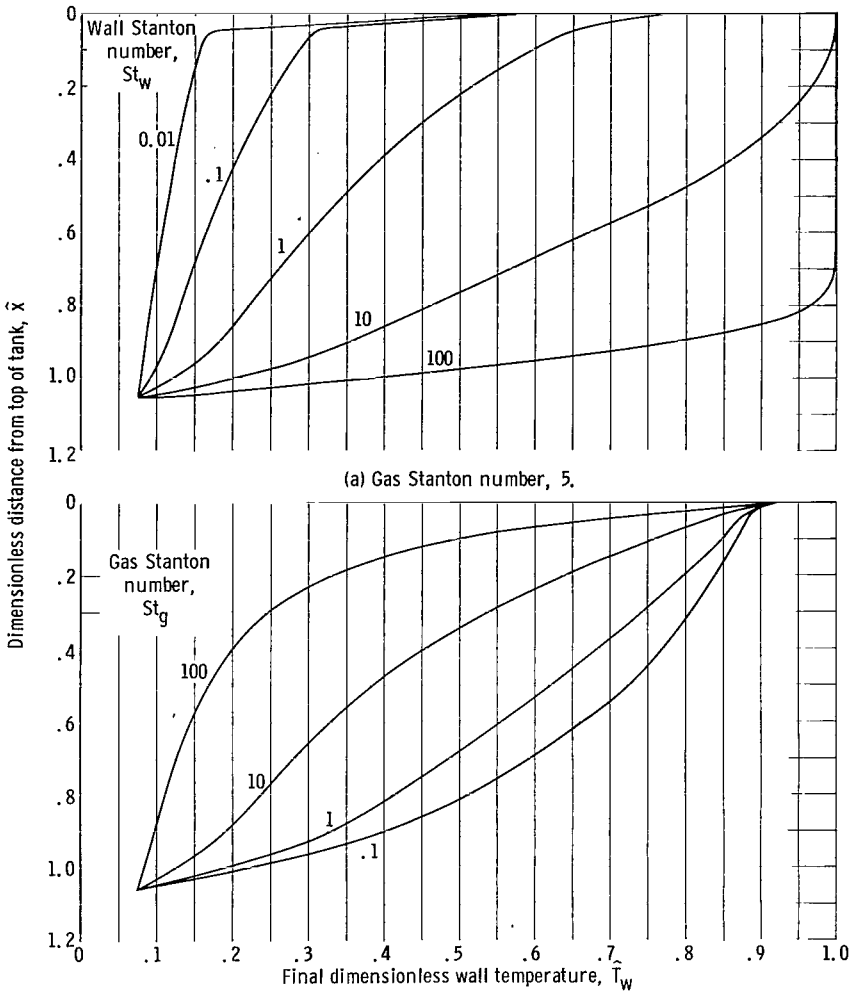

(a) Gas Stanton number, 5.

(b) Wall Stanton number, 2.5.

Figure 17. - Final dimensionless wall temperature at end of outflow. Dimensionless initial ullage height, 0.0526; dimensionless interface temperature, 0.074; dimensionless time from start of outflow, 1.

sometimes used in simple analyses of the pressurization problem, that a linear variation of temperature can be used as a good approximation to the actual temperature distribution, is evidently not valid over the entire range of Stanton numbers.

COMPARISON OF PREDICTED AND EXPERIMENTAL VALUES OF MASS RATIO

In obtaining the reference Stanton number map (fig. 3, p. 7) many simplifications were made. The foregoing results indicate, however, that the most important effects on

TABLE I. - VALUES USED FOR COMPUTATION OF STANTON NUMBERS FOR EXPERIMENTS OF REFERENCE 2

[Wall thickness, 0.026 ft; wall density, 500 lb/cu ft; tank radius, 1.13 ft.]

Run	Average wall specific heat, $\bar{c}_w$, Btu/(lb)(°R)	Gas density, ρ_g, lb/cu ft	Gas specific heat, c_p, Btu/(lb)(°R)	Outflow time, t_f, sec	Heat-transfer coefficient, h×3600, Btu/(hr)(ft²)(°R)
1	0.0730	0.0573	2.98	350	13.75
2	.0725	.0584		93	12.25
3	.0730	.0204		284	7.09
4	.0735	.0206		101	6.67
5	.0423	.1110		95	11.34
6	.0800	.0120		88	5.13
7	.0738	.1120	1.24	355	12.31
8	.0738	.1120		90	11.15
9	.0316	.2790		100	10.45
10	.0792	.0240		309	5.25

the pressurant mass ratio are probably included in the map. To test this experimentally, the liquid hydrogen outflow experiments that were used for comparison in reference 1 will be considered here. These experiments (reported in refs. 2 and 3) cover a range of tank pressure, outflow rate, and inlet gas temperature, and include, in some instances, significant transients in the inlet gas temperature.

Reference 2 Data

In reference 2 the authors report some of the results of a systematic series of liquid hydrogen expulsion experiments with a cylindrical tank. The tank used was 27 inches in diameter and 89 inches in overall length with dished head ends. A gas diffuser was used at the inlet. The tank was made of 5/16-inch 304 stainless-steel plate and was vacuum jacketed. The internal instrumentation, described in detail in reference 2, provided a relatively significant heat sink in some of the tests.

Ten experimental runs (not all of which were published in ref. 2) were used in reference 1 to compare calculated and experimental mass requirements. These runs covered a wide range of values of temperature, pressure, and outflow rate. Four of the runs used helium as the pressurizing gas. The detailed data are given in reference 1. Table I shows the data needed for the calculation of modified gas and wall Stanton numbers for each case. The values of heat-transfer coefficient are average values determined from

TABLE II. - COMPARISON OF CALCULATED AND EXPERIMENTAL MASS RATIOS FOR EXPERIMENTS OF REFERENCE 2

Run	Dimensionless gas Stanton number, St_g	Dimensionless wall Stanton number, St_w	Mass ratio, m/m_i		Percent difference
			Figure 3	Experimental	
1	6.93	1.41	2.58	2.97	-13.1
2	1.61	.34	1.77	2.12	-16.5
3	8.14	.59	3.09	3.88	-20.3
4	2.70	.20	2.20	2.66	-17.3
5	.88	.54	1.47	1.53	-3.9
6	3.10	.12	2.37	3.08	-23.0
7	7.73	1.27	2.73	3.24	-15.7
8	1.78	.29	1.86	2.14	-13.1
9	.74	.71	1.38	1.41	-2.1
10	13.39	.44	3.92	5.10	-23.2

each experiment. The wall specific heat is the integrated average value indicated in figure 2 (p. 7).

When the values in table I were used, the modified gas and wall Stanton numbers were computed from equations (19) and (21), and the values of mass ratio were then found from figure 3. Table II lists the computed values of modified Stanton numbers and the resulting values of mass ratio. Also listed are the experimental values of mass ratio in each case and the percent difference between the calculated and experimented values.

The agreement shown in table II is not as good as might be expected from the parametric analysis. The explanation for this probably lies in the large heat sink provided by the internal instrumentation in the experiments of reference 2. The effect of the heat sink on mass ratio, which is not accounted for in figure 3, was shown to be significant in the calculations of reference 1. In that reference the effect of the heat sink on the mass requirement was determined from an estimated value of heat flow to the internal hardware. If the experimental values of m/m_i given in table II are adjusted by these calculated amounts, the results are those given in table III. With the adjustment for the heat flow to the internal hardware, the agreement of the calculated and experimental values is much better. The average absolute value of the difference for the 10 cases is 6.2 percent. It is clear here, as it was in reference 1, that neglecting internal heat flow can cause significant error in the calculated results.

Reference 3 Data

Reference 3 reports the results of liquid hydrogen expulsion experiments using a 40-inch-diameter cylindrical test tank 100 inches in overall length. The test tank was 0.090-inch-thick stainless steel and was enclosed in a 60-inch-diameter vacuum-tight carbon-steel tank. A gas diffuser was in the top and an antivortex baffle was in the bottom. Perforated conical slosh baffles were located at various axial distances. The heat sink effect of the internal hardware could not be estimated from the data reported in reference 3.

TABLE III. - COMPARISON OF CALCULATED AND ADJUSTED EXPERIMENTAL MASS RATIOS FOR EXPERIMENTS OF REFERENCE 2

Run	Mass ratio, m/m_i		Percent difference
	Figure 3	Adjusted experimental	
1	2.58	2.76	-6.5
2	1.77	1.84	-3.8
3	3.09	3.31	-6.7
4	2.20	2.25	-2.2
5	1.47	1.35	8.9
6	2.37	2.56	-7.4
7	2.73	2.86	-4.5
8	1.86	1.93	-3.6
9	1.38	1.25	10.4
10	3.92	4.25	-7.8

TABLE IV. - VALUES USED FOR COMPUTATION OF STANTON NUMBERS FOR EXPERIMENTS OF REFERENCE 3

[Wall thickness, 0.0075 ft; wall density, 500 lb/cu ft; tank radius, 1.67 ft.]

Run	Average wall specific heat, $\bar{c}_w$, $\frac{Btu}{(lb)(^oR)}$	Gas density, ρ_g, $\frac{lb}{cu\ ft}$	Gas specific heat, c_p, $\frac{Btu}{(lb)(^oR)}$	Outflow time, t_f, sec	Heat-transfer coefficient, h×3600, $\frac{Btu}{(hr)(ft^2)(^oR)}$
1	0.0475	0.0283	2.67	89	11.5
2	.0730	.0171	2.98	103	[a]12.0
3	.0475	.0289	2.67	120	11.3
4		.0289	2.67	87	12.0
5		.0566	1.24	99	12.1
6		.0280	2.67	111	11.8
7		.0286	2.67	97	11.7
8		.0286	2.67	105	13.9

[a]Estimated value - not given in reference 3.

TABLE V. - COMPARISON OF CALCULATED AND EXPERIMENTAL MASS RATIOS FOR EXPERIMENTS OF REFERENCE 3

Run	Mass ratio, m/m_i		Percent difference
	Figure 3	Experimental	
1	1.72	1.54	11.7
2	2.14	2.16	-.9
3	1.79	1.61	11.2
4	1.71	1.68	1.8
5	1.81	1.69	7.1
6	1.80	1.71	5.3
7	1.75	1.59	10.0
8	1.83	1.69	8.3

Nine tests were reported in reference 3 for which the system vacuum was maintained. Of these nine tests (all of which were used in the comparisons of calculated and experimental results in ref. 1) only eight are considered here. It was necessary to omit the one that used hydrogen to pressurize the tank but had helium in the ullage initially. Such an arrangement is not covered in the results of figure 3. The cases used cover two values of inlet gas temperature and a range of initial ullage volumes up to about 20 percent. The outflow time and tank pressure vary slightly for the eight cases. Helium was used as a pressurizing gas in one case. Sloshing was induced in all but one case. Complete data for the calculation are given in reference 1.

Table IV shows the data used for the calculation of the modified Stanton numbers for the eight experiments. The values of h are experimental average values as they were in table I.

When the values in table IV were used, the modified Stanton numbers were computed as before and the mass

TABLE VI. - COMPARISON OF MASS RATIOS FOR COMPUTED VALUES OF AVERAGE HEAT-TRANSFER COEFFICIENT

Run	Heat-transfer coefficient, h, equation (26)	Mass ratio, m/m_i		Percent difference
		Figure 3	Experimental	
Reference 1 data				
1	16.4	2.75	2.76	-0.4
2	16.5	1.90	1.84	3.3
3	8.35	3.25	3.31	-1.8
4	8.40	2.35	2.25	4.4
5	18.5	1.60	1.35	18.5
6	6.23	2.45	2.56	-4.3
7	12.6	2.77	2.86	-3.1
8	12.6	1.91	1.93	-1.0
9	17.7	1.45	1.25	16.0
10	4.78	3.80	4.25	-10.4
Reference 2 data				
1	7.9	1.60	1.54	3.9
2	7.4	1.95	2.16	-9.7
3	8.1	1.70	1.61	5.6
4	8.1	1.55	1.68	-7.7
5	6.9	1.65	1.69	-2.4
6	7.7	1.65	1.71	-3.5
7	8.0	1.62	1.59	1.9
8	7.9	1.68	1.69	-.6

ratio found from figure 3. Table V gives the resulting Stanton numbers and mass ratios and the comparable experimental values. The average absolute difference between calculated and experimental values is 7.0 percent.

For data of references 2 and 3, therefore, the agreement is quite good when proper allowance is made for internal heat sinks where these are important. This result bears out the implication of the parametric analysis that the reference Stanton number map contains the important factors influencing the mass ratio. It appears therefore that figure 3 can be used to obtain rapid approximate predictions of mass ratio providing a suitable value of heat-transfer coefficient can be obtained.

Heat-Transfer Coefficient

The values of heat-transfer coefficient h used in determining Stanton numbers in the previous section were experimental values. For design use of figure 3 to obtain values of mass ratio, h must be estimated by some other means. A simple way to do this is to use the free convection formula (ref. 4):

$$h = 0.13 \frac{k}{\ell} (Gr \times Pr)^{0.333} \tag{26}$$

where the properties are evaluated at the characteristic temperature T_g. The values of h obtained using equation (26) for the 18 experiments treated in the previous section are shown in table VI along with the experimental average values. Also shown in this table are the values of m/m_i obtained from figure 3 by using the reference Stanton numbers calculated from the analytical values of h. The experimental values of m/m_i are repeated from tables III and V and the final column gives the percent difference between calculated and experimental values of mass ratio. The average absolute difference is less than 6 percent.

These results indicate that, at least for these experiments, the simple scheme described for determining h is adequate for predicting mass ratios.

SUMMARY OF RESULTS

A simple model was postulated in NASA Technical Note D-2585 for the problem of tank pressurization during outflow. In the present report the equations derived in the aforementioned report were further simplified and put into dimensionless form. An examination of the dimensionless equations and a large number of numerical solutions led to the following results:

1. The pressurant mass ratio (collapse factor) depends principally on two dimensionless quantities having the form of modified Stanton numbers, one associated with the gas and one with the tank wall. These numbers are functions of tank geometry, outflow time, inlet gas properties, tank wall properties, and an average value of heat-transfer coefficient.

2. Other parameters that influence the pressurant mass ratio to a lesser degree are the inlet gas temperature, the ratio of liquid surface temperature to inlet gas temperature, and the ratio of initial ullage volume to the total volume of liquid outflow. The influence of these parameters is negligible in many cases.

3. A reference Stanton number map is given from which rapid approximate values of mass ratio can be found from specified values of reference Stanton numbers. To obtain Stanton numbers for a particular problem it is necessary to estimate an average value of the heat-transfer coefficient.

4. For a variety of experimental data the reference Stanton number map was used to predict values of mass ratio; average values of heat-transfer coefficient obtained from the experiments were used. The predicted values of mass ratio agreed with the experimental values to within 7 percent, on the average.

5. Average heat-transfer coefficients were calculated for the experiments by using a free convection formula with properties evaluated at the inlet gas temperature. The mass ratios predicted using these calculated values of heat-transfer coefficient agreed with experimental values to within 6 percent, on the average.

Lewis Research Center,
National Aeronautics and Space Administration,
Cleveland, Ohio, December 22, 1964.

APPENDIX - SYMBOLS

c_p specific heat of gas at constant pressure, Btu/(lb)(^{o}R)

c_w specific heat of tank wall, Btu/(lb)(^{o}R)

$\bar{c}_w$ integrated average wall specific heat (eq. (23), Btu/(lb)(^{o}R)

$\hat{c}_w$ dimensionless wall specific heat, $\bar{c}_w/c_w$

Gr Grashof number

h heat-transfer coefficient, Btu/(sq ft)(sec)(^{o}R)

L height of ullage space, ft

$\hat{L}$ dimensionless height of ullage space, $L/(L_f - L_o)$

L_f height of ullage space at end of outflow, ft

$\hat{L}_f$ dimensionless final ullage height, $L_f/(L_f - L_o)$

L_o height of ullage space at start of outflow, ft

$\hat{L}_o$ dimensionless initial ullage height, $L_o/(L_f - L_o)$

ℓ_w tank wall thickness, ft

$\hat{\ell}_w$ dimensionless tank wall thickness, $\ell_w/(L_f - L_o)$

M molecular weight

m mass of pressurant added during outflow, lb

m_i ideal mass of pressurant added (eq. (25)), lb

P pressure in tank, lb/sq ft

Pr Prandtl number

R universal gas constant, ft-lb/(^{o}R)(lb-mole)

r tank radius, ft

$\hat{r}$ dimensionless tank radius, $r/(L_f - L_o)$

St_g dimensionless gas Stanton number (eq. (19))

St_w dimensionless wall Stanton number (eq. (20))

T temperature of ullage gas, ^{o}R

$\hat{T}$ dimensionless temperature of ullage gas, T/T_g

T_g inlet gas temperature, ^{o}R

T_L liquid surface temperature, ^{o}R

$\hat{T}_L$ dimensionless liquid surface temperature, T_L/T_g

T_w tank wall temperature, ^{o}R

$\hat{T}_w$ dimensionless tank wall temperature, T_w/T_g

t time from start of outflow, sec

$\hat{t}$ dimensionless time from start of outflow, t/t_f

t_f time at end of outflow, sec

u velocity of ullage gas, ft/sec

$\hat{u}$ dimensionless velocity of ullage gas, u/u_L

u_L velocity of liquid surface, ft/sec

x space coordinate measured vertically downward from top of tank, ft

$\hat{x}$ dimensionless space coordinate, $x/(L_f - L_o)$

ρ_g ullage gas density, lb/cu ft

ρ_w tank wall density, lb/cu ft

REFERENCES

1. Roudebush, William H.: An Analysis of the Problem of Tank Pressurization During Outflow. NASA TN D-2585, 1965.
2. Gluck, D. F.; and Kline, J. F.: Gas Requirements in Pressurized Transfer of Liquid Hydrogen. Advances in Cryogenic Engineering, vol. 7, 1962.
3. Main Propellant Tank Pressurization System Study and Test Program. Lockheed-Georgia Co. Rep ER-5238, Aug. 1961.
4. McAdams, William H.: Heat Transmission. Third Edition, McGraw-Hill, 1964, p. 172.

NASA-Langley, 1965 E-2727

"The aeronautical and space activities of the United States shall be conducted so as to contribute . . . to the expansion of human knowledge of phenomena in the atmosphere and space. The Administration shall provide for the widest practicable and appropriate dissemination of information concerning its activities and the results thereof."

—NATIONAL AERONAUTICS AND SPACE ACT OF 1958

NASA SCIENTIFIC AND TECHNICAL PUBLICATIONS

TECHNICAL REPORTS: Scientific and technical information considered important, complete, and a lasting contribution to existing knowledge.

TECHNICAL NOTES: Information less broad in scope but nevertheless of importance as a contribution to existing knowledge.

TECHNICAL MEMORANDUMS: Information receiving limited distribution because of preliminary data, security classification, or other reasons.

CONTRACTOR REPORTS: Technical information generated in connection with a NASA contract or grant and released under NASA auspices.

TECHNICAL TRANSLATIONS: Information published in a foreign language considered to merit NASA distribution in English.

TECHNICAL REPRINTS: Information derived from NASA activities and initially published in the form of journal articles.

SPECIAL PUBLICATIONS: Information derived from or of value to NASA activities but not necessarily reporting the results of individual NASA-programmed scientific efforts. Publications include conference proceedings, monographs, data compilations, handbooks, sourcebooks, and special bibliographies.

Details on the availability of these publications may be obtained from:

SCIENTIFIC AND TECHNICAL INFORMATION DIVISION

NATIONAL AERONAUTICS AND SPACE ADMINISTRATION

Washington, D.C. 20546